Bioconjugate Chemistry

Article

pubs.acs.org/bc

PEG-Derivatized Embelin as a Dual Functional Carrier for the Delivery of Paclitaxel

Yixian Huang,[#,†,‡] Jianqin Lu,[#,†,‡] Xiang Gao,[†,‡] Jiang Li,[†,‡] Wenchen Zhao,[‡] Ming Sun,[§] Donna Beer Stolz,[§] Raman Venkataramanan,[‡] Lisa Cencia Rohan,[‡,∥] and Song Li*[,†,‡]

[†]Center for Pharmacogenetics, [‡]Department of Pharmaceutical Sciences, School of Pharmacy; [§]Department of Cell Biology and Physiology, School of Medicine; [∥]Magee Women's Research Institute, University of Pittsburgh, Pittsburgh, Pennsylvania 15261, United States

Supporting Information

ABSTRACT: Embelin, identified primarily from the *Embelia ribes* plant, has been shown to be a natural small molecule inhibitor of X-linked inhibitor of apoptosis protein (XIAP). It is also a potent inhibitor of NF-κB activation, which makes it a potentially effective suppressor of tumor cell survival, proliferation, invasion, angiogenesis, and inflammation. However, embelin itself is insoluble in water, which makes it unsuitable for in vivo applications. In this work, we developed a novel micelle system through conjugating embelin to a hydrophilic polymer, poly(ethylene glycol) 3500 ($PEG_{3.5K}$) through an aspartic acid bridge. The $PEG_{3.5k}$-$embelin_2$ ($PEG_{3.5k}$-EB_2) conjugate readily forms micelles in aqueous solutions with a CMC of 0.0205 mg/mL. Furthermore, $PEG_{3.5k}$-EB_2 micelles effectively solubilize paclitaxel (PTX), a model hydrophobic drug used in this study. Both drug-free and drug-loaded micelles were small in size (20−30 nm) with low polydispersity indexes. In vitro cytotoxicity studies with several tumor cell lines showed that $PEG_{3.5k}$-EB_2 is comparable to embelin in antitumor activity and synergizes with PTX at much lower doses. Our results suggest that PEG-derivatized embelin may represent a novel and dual-functional carrier to facilitate the in vivo applications of poorly water-soluble anticancer drugs such as PTX.

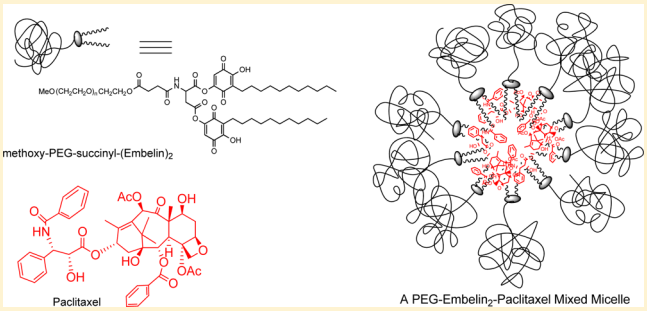

INTRODUCTION

Low water solubility, high protein binding, and relatively short half-life are major problems in clinical applications of many potent anticancer drugs such as paclitaxel (PTX).[1,2] Currently, a variety of drug delivery systems such as liposomes, dendrimers, microcapsules, and polymeric micelles have been developed to address these problems and further to promote sustained, controlled, and targeted delivery of poorly water-soluble anticancer drugs.[3] Of all these delivery systems, polymeric micelles have gained considerable attention as a versatile nanomedicine platform due to their technical ease, high biocompatibility, and high efficiency in drug delivery.[4,5] Polymer micelles have been demonstrated to improve the aqueous solubility of chemotherapeutic agents and prolong their in vivo half-lives, owing to the steric hindrance provided by a hydrophilic shell.[4,5] Moreover, compared with other delivery systems, micelles show advantages in passive tumor targeting through the leaky vasculature via the enhanced permeability and retention (EPR) effect due to their small size ranging from 10 to 100 nm.[6,7] Favorable drug biodistribution and improved therapeutic index can be achieved by using the micelle delivery system.[3,4] However, most of the polymeric systems use "inert" excipients that lack therapeutic activity. The presence of large amounts of carrier materials not only adds to the cost, but also imposes additional safety issues.[8]

One of the most sophisticated designs of drug delivery systems is that in which the components forming the carriers can also have therapeutic effects. The carrier materials may be capable of counteracting the side effects caused by the loaded anticancer drugs.[9] Also, it is possible that the carrier may collaborate with the loaded drug to achieve synergistic effects to better treat the tumor.[5] However, the strategy of using highly water-insoluble drugs themselves as the hydrophobic region of polymeric micelles is rarely reported. One example is the pegylated vitamin E, D-α-tocopheryl poly(ethylene glycol) succinate (Vitamin E TPGS or TPGS).[10−12] Vitamin E shows antitumor activity against a number of types of cancers through various mechanisms such as induction of apoptosis, inhibition of tumor cell proliferation and differentiation, suppression of nuclear factor-kappa B (NF-κB) activation, and so forth.[13,14] The pegylated vitamin E is a highly water-soluble amphiphilic molecule comprising a lipophilic alkyl tail and a hydrophilic polar head portion. In addition to its antitumor activity, it is

Received: February 2, 2012
Revised: June 4, 2012
Published: June 9, 2012

dx.doi.org/10.1021/bc3000468 | *Bioconjugate Chem.* 2012, 23, 1443−1451

Scheme 1. Synthesis of $PEG_{3.5K}$-EB_2[a]

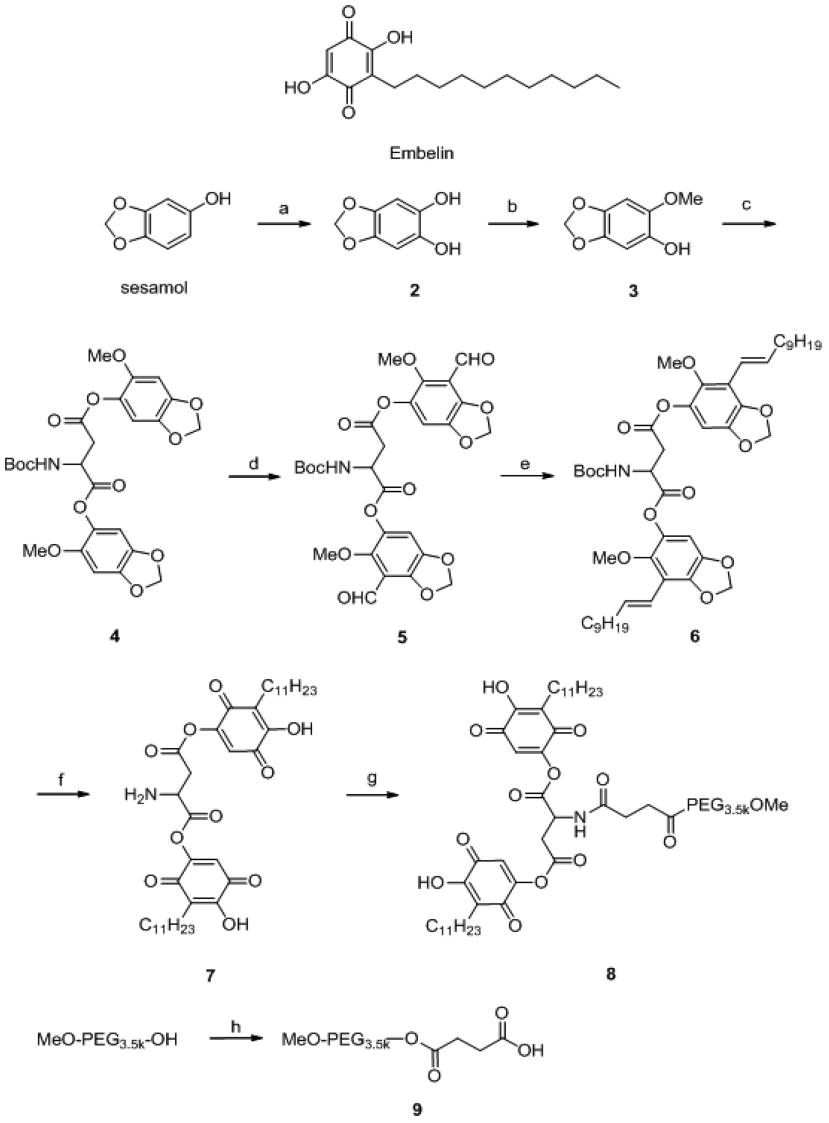

[a]Conditions: (a) water, Fremy's salt, KH_2PO_4, 5 min; $Na_2S_2O_4$, 30 min; (b) water, Mel NaOH: l h; (c) Boc-Aspartic acid DCC, DMAP, CH_2Cl_2, overnight; (d) MeCN, DMF, $POCl_3$; (e) THF, LiHMDS 2 M in THF, decyltriphenylphosphonium bromide, 2 h (f) (1) MeOH, H_2, Pd/C; (2) MeCN, CAN; (3) dioxane, HCl, 2 h; (g) CH_2Cl_2, DCC, DMAP, **9**; overnight; (h) succinic anhydride, DMAP, CH_2Cl_2, 2 days.

effective in solubilizing various hydrophobic drugs such as PTX. Synergistic actions between the TPGS-based carrier and delivered anticancer agents have been reported.[5]

In this study, we report the development of PEG-derivatized embelin as another novel and dual-functional carrier for delivery of poorly water-soluble anticancer drugs. Embelin is a naturally occurring alkyl-substituted hydroxyl benzoquinone compound and a major constituent of *Embelia ribes* BURM. It has been shown to possess antidiabetic, anti-inflammatory, and hepatoprotective activities.[15−17] Embelin also shows antitumor activity in various types of cancers.[15,18−21] One major mechanism involves the inhibition of the activity of X-linked inhibitor of apoptosis protein (XIAP).[22] XIAP is overexpressed in various types of cancers cells, particularly drug-resistant cancer cells, and inhibition of XIAP has been explored as a new approach for the treatment of cancers.[23,24] XIAP plays a minimal role in normal cells, and therefore, embelin shows significantly less toxicity on normal cells. Embelin also downregulates the expression of survivin, XIAP, IAP1/2, TRAF1, cFLIP, Bcl-2, and Bcl-x_L through the inhibition of NF-κB activation.[25] Embelin is poorly water-soluble, and PEG modification was originally explored by us as an approach to increase its solubility. Interestingly, PEG-derivatized embelin forms micelles that are highly efficient in solubilizing other compounds such as PTX. Preparation of PEG-derivatized embelin can be readily achieved with commercially available embelin. In addition, we have developed an efficient synthesis strategy to prepare PEG−embelin conjugate. Our in vitro studies showed that PEG−embelin has similar activity to free embelin with IC_{50} in the low micromolar range. More importantly, PEG−embelin synergizes with PTX at much lower doses (~nM) in a number of cancer cell lines tested.

EXPERIMENTAL PROCEDURES

Materials. Paclitaxel (98%) was purchased from AK Scientific. Inc. (CA, USA). 2,5-Dihydroxy-3-undecyl-1,4-benzoquinone (embelin 98%) was purchased from 3B Scientific Corporation (IL, USA). Dulbecco's phosphate buffered saline

dx.doi.org/10.1021/bc3000468 | *Bioconjugate Chem.* 2012, 23, 1443−1451

(DPBS) was purchased from Lonza (MD, USA). Methoxy-$PEG_{3,500}$-OH, dimethyl sulfoxide (DMSO), 3-(4,5-dimethylthiazol-2-yl)-2,5-diphenyl tetrazolium bromide (MTT), trypsin-EDTA solution, Triton X-100, and Dulbecco's Modified Eagle's Medium (DMEM) were all purchased from Sigma-Aldrich (MO, USA). Fetal bovine serum (FBS) was purchased from Gibco Life Technologies (AG, Switzerland). Penicillin−streptomycin solution was from Invitrogen (NY, USA). All solvents used in this study were HPLC grade.

Cell Culture. DU145 and PC3 are two androgen-independent human prostate cancer cell lines. MDA-MB-231 is a human breast adenocarcinoma cell line. 4T1 is a mouse metastatic breast cancer cell line. All cell lines were cultured in DMEM containing 10% FBS and 1% penicillin−streptomycin in a humidified environment at 37 °C with 5% CO_2.

Synthesis of $PEG_{3.5K}$-Embelin$_2$ ($PEG_{3.5K}$-EB_2). Scheme 1 shows the synthesis sequence of $PEG_{3.5K}$-EB_2 conjugate. Synthesis of the intermediates and structural characterizations are detailed below.

Compound **2**: Sesamol (1.52 g, 24 mmol) in 30 mL of methanol was added to a rapidly stirred solution of Fremy's salt (7.96 g, 30 mmol) and 5.49 g (40 mmol) of KH_2PO_4 in 400 mL water at 5 °C. The color of the solution changed from light brown to bright yellow within 5 min. The mixture was stirred for another 30 min and then extracted with 4 × 40 mL of ethyl acetate. The ethyl acetate phase was treated with a solution of $Na_2S_2O_4$ (9.0 g, 52 mmol) in water (30 mL), and the yellow color changed to a colorless solution. The organic layer was acidified with HCl (1 N), extracted with ethyl acetate (3 × 30 mL), washed with water (20 mL), dried with anhydrous $MgSO_4$, and concentrated to give 1.1 g (65%) of **2** as a light pink solid. ^{1}H NMR($(CD_3)_2CO$): δ 7.49 (s, 2H), 6.45 (s, 2H), 5.79 (s, 2H).

Compound **3**: A solution of **2** (1.54 g, 10 mmol) in water (30 mL) was treated with NaOH (0.4 g, 10 mmol) while the flask was kept in an ice bath. The reaction mixture was stirred for 15 min after which MeI (1.41 g, 10 mmol) was added dropwise. The reaction mixture was then heated under reflux for 1 h, allowed to cool down to room temperature, and the solvent was removed via a rotary evaporator. The crude product was purified by flash chromatography with silica gel (ethyl acetate:petroleum ether, 1:5) and pure **3** was obtained as an amber oil with a yield of 99% (1.68 g). ^{1}H NMR($CDCl_3$): δ 6.11 (m, 2H), 5.88 (s, 2H), 5.35 (s, 1H), 3.72 (s, 3H).

Compound **4**: To a solution of *N*-(*tert*-butoxycarbonyl)-L-aspartic acid (Boc-Asp-OH) (2.33 g, 10 mmol) in CH_2Cl_2 (40 mL) was added dicyclohexylcarbodiimide (DCC) (6.2 g, 30 mmol), 4-dimethyamineopyridine (DMAP) (0.61 g, 5 mmol), and compound **3** (3.36 g, 20 mmol) at room temperature. The reaction mixture was stirred overnight at room temperature. After the reaction was completed, 100 mL Et_2O was added to the mixture. The mixture was filtered to remove the insoluble DCU byproduct and the organic phase of the filtrate was concentrated under vacuum. The resulting residue was purified by silica gel flash chromatography (MeOH:CH_2Cl_2, 1:10) to give pure **4** as an oil in 62% yield (3.31 g). ^{1}H NMR ($CDCl_3$): δ 6.11 (m, 4H), 5.88 (m, 4H), 5.40 (m, 1H), 4.65 (m, 1H), 3.74 (s, 3H), 3.72 (s, 3H), 2.88 (m, 1H), 2.64 (m, 1H), 1.42 (s, 9H). ESI-MS m/z 534.2 ($[M+H]^+$).

Compound **5**: To a solution of **4** (5.33 g, 10 mmol) in acetonitrile (MeCN, 10 mL) at 0−5 °C, dry dimethylformamide (DMF) (0.73 g, 10 mmol) and $POCl_3$ (1.78 g, 11 mmol) were added with constant stirring over 0.5 h. The salt formed was filtered, washed with cold MeCN, dissolved in 20 mL of water, heated at 50 °C for 0.5 h, and then cooled. The mixture was extracted with 3 × 40 mL of CH_2Cl_2, and the combined organic phase was washed with brine, dried over anhydrous Na_2SO_4, and concentrated in vacuum. The crude residue was purified by silica gel flash chromatography (MeOH:CH_2Cl_2, 1:10) to give pure **5** as an oil in 80% yield (4.82 g). ^{1}H NMR ($CDCl_3$): δ 10.21 (s, 1H), 10.18 (s, 1H), 6.65 (m, 2H), 5.92 (m, 4H), 5.37 (m, 1H), 4.51 (m, 1H), 3.75 (s, 3H), 3.72 (s, 3H), 2.85 (m, 1H), 2.60 (m, 1H), 1.40 (s, 9H). ESI-MS m/z 590.5 ($[M+H]^+$).

Compound **6**: A solution of sodium bis(trimethylsilyl)amide (12 mL, 2 M solution in THF) was added dropwise to a stirred solution of decanyltriphenylphosphonium bromide (9.67 g, 20 mmol) in 40 mL THF at room temperature. The resulting mixture was stirred for 30 min at room temperature and then cooled to −78 °C. To this mixture was added compound **5** (6.03 g, 10 mmol). The reaction mixture was stirred for 2 h at −78 °C and then warmed up to room temperature. The reaction mixture was quenched with saturated solution of NH_4Cl, extracted with ethyl acetate. The combined organic layer was washed with brine, dried over anhydrous Na_2SO_4, and concentrated in vacuum. The crude residue was purified by silica gel flash chromatography (MeOH:CH_2Cl_2, 1:10) to give pure **6** as an oil in 90% yield. ^{1}H NMR ($CDCl_3$): δ 6.48 (m, 2H), 6.39 (m, 2H), 6.02 (m, 2H), 5.86 (m, 4H), 5.35 (m, 1H), 4.53 (m, 1H), 3.75 (s, 3H), 3.72 (s, 3H), 2.83 (m, 1H), 2.61 (m, 1H), 2.15 (m, 4H), 1.40 (s, 9H), 1.29 (m, 28H), 0.91 (m, 6H). ESI-MS m/z 838.4 ($[M+H]^+$).

Compound **7**: The double bond in compound **6** (8.37 g, 10 mmol) was saturated by catalytic hydrogenolysis with Pd/C (10%, 500 mg) under H_2 (1 atm) in a methanol solution (50 mL) at room temperature for 2 h. The solution was filtered to remove Pd/C and concentrated under vacuum. The resulting product was then dissolved in the solution of 10 mL of water, 10 mL MeCN, and 20 mmol CAN (ammonium ceric nitrate) (10.96 g). The mixture was cooled to 0 °C and stirred for another 2 h. MeCN was then removed via evaporation under reduced pressure, 100 mL CH_2Cl_2 was added to the remaining aqueous solution. The organic phase was washed with brine and then concentrated under vacuum. 10 mL dioxane and 10 mL HCl were then added to the residue. The mixture was stirred at room temperature for 24 h. The reaction mixture was quenched with saturated solution of $NaHCO_3$ and extracted with ethyl acetate. The organic layer was washed with brine, dried over anhydrous Na_2SO_4, and concentrated under vacuum. The crude product was purified by silica gel flash chromatography (MeOH:CH_2Cl_2, 1:10) to give pure **7** as an oil in 42% yield (2.89 g). ^{1}H NMR($CDCl_3$): δ 8.16 (m, 2H), 6.75 (m, 2H), 5.35 (m, 2H), 4.53 (m, 1H), 2.85 (m, 1H), 2.60 (m, 1H), 2.43 (m, 4H), 1.25 (m, 36H), 0.89 (m, 6H). ESI-HRMS calcd for $C_{38}H_{55}NO_{10}Na$ ($[M+Na]^+$) 708.4766, found 708.4747.

Compound **8**: A solution of MeO-$PEG_{3.5k}$-CO_2H (3.5 g, 1 mmol) in CH_2Cl_2 (5 mL) was treated with DCC (0.41 g, 2 mmol), DMAP (0.12 g, 1 mmol), and compound **7** (689 mg, 1 mmol) at room temperature. The reaction mixture was stirred overnight. After the reaction was completed, 100 mL of Et_2O was added and the mixture was filtered and concentrated under vacuum. The resulting residue was purified by silica gel flash chromatography (MeOH:CH_2Cl_2, 1:10) to give pure **8** ($PEG_{3.5K}$-EB_2) as a wax solid in ∼50% yield (2.1 g). ^{1}H NMR ($CDCl_3$): δ 8.14 (m, 2H), 6.72 (m, 2H), 5.57 (m, 1H),

dx.doi.org/10.1021/bc3000468 | *Bioconjugate Chem.* 2012, 23, 1443−1451

4.98 (m, 1H), 3.35 (s, 3H), 2.60 (m, 10H), 1.25 (m, 36H), 0.89 (m, 6H).

Formation of Micelles. PTX-solubilized micelles were prepared by the following method. PTX (10 mM in chloroform) was added to $PEG_{3.5K}$-EB_2 (10 mM in chloroform) with various carrier/drug ratios. The organic solvent was first removed by nitrogen flow to form a thin film of drug/carrier mixture. The film was further dried under high vacuum for 2 h to remove any traces of remaining solvent. Drug-loaded micelles were formed by suspending the film in DPBS. The drug-free micelles were similarly prepared as described above.

Measurement of Size and Zeta Potential. Zetasizer (Zetasizer Nano ZS instrument, Malvern, Worcedtershire, UK) was used to measure the particle size and zeta potential of drug-free and drug-loaded micelles. Micelles were stored at 4 °C, and the samples were tested for changes in particle size and size distribution.

Determination of PTX Loading Efficiency. PTX-solubilized micelles were prepared at an input PTX concentration of 1.07, 2.14, and 3.21 mg/mL, respectively. Aliquots of samples were filtered through 0.45 μm PVDF syringe filter. PTX in the filtered and nonfiltered micelles was extracted using methanol and measured by high-performance liquid chromatography (HPLC, Waters). A reverse phase column (C18) was employed. The detection was performed by using UV detector at 227 nm, 70% methanol as a mobile phase, flow rate at 1.0 mL/min. Drug loading capacity (DLC) and drug loading efficiency (DLE) were calculated according to the following formula:

$$\mathrm{DLC}(\%) = [\text{weight of drug used}/(\text{weight of polymer} + \text{drug used})] \times 100\%$$

$$\mathrm{DLE}(\%) = (\text{weight of loaded drug}/\text{weight of input drug}) \times 100\%$$

Determination of the Critical Micelle Concentration (CMC). The CMC of $PEG_{3.5K}$-EB_2 was determined by employing pyrene as a fluorescence probe.[26] A drug-free micelle solution in DPBS (2.5 mg/mL) was prepared via solvent evaporation method. A series of 2-fold dilutions was then made with $PEG_{3.5K}$-EB_2 concentrations ranging from 7.63×10^{-5} to 2.5 mg/mL. At the same time, aliquots of 50 μL of 4.8×10^{-6} M pyrene in chloroform were added into 15 separate vials. The chloroform was first removed by nitrogen flow to form a thin film. The film was further dried under high vacuum for 2 h to remove any traces of remaining solvent. Then, the preprepared micelle solutions (400 μL in DPBS) of varying $PEG_{3.5K}$-EB_2 concentrations were added to the pyrene film to obtain a final pyrene concentration of 6×10^{-7} M for each vial. The solutions were kept on a shaker at 37 °C for 24 h to reach equilibrium before fluorescence measurement. The fluorescence intensity of samples was measured at the excitation wavelength of 334 nm and emission wavelength of 390 nm by Synergy H1 Hybrid Multi-Mode Microplate Reader (Winooski, VT). The CMC is determined from the threshold concentration, where the sharp increase in pyrene fluorescence intensity is observed.

Transmission Electron Microscope (TEM). The morphology of micelles was observed on a Jeol 1011 transmission electron microscope (TEM). The aqueous micelle solution (1.0 mg/mL) was added onto copper grids coated with Formvar, and then stained with 1% uranyl acetate. The sample processing and imaging were performed at room temperature.

Hemolysis Assay. Fresh blood samples were collected through cardiac puncture from rats. Ten milliliters of blood was added with EDTA-Na_2 immediately to prevent coagulation. Red blood cells (RBCs) were separated from plasma by centrifugation at 1500 rpm for 10 min at 4 °C. The RBCs were washed three times with 30 mL ice-cold DPBS. RBCs were then diluted to 2% w/v with ice-cold DPBS and utilized immediately for the hemolysis assay. One milliliter of diluted RBC suspension was treated with various concentrations (0.2 and 1.0 mg/mL) of $PEG_{3.5k}$-EB_2 and PEI, respectively, and then incubated at 37 °C in an incubator shaker for 4 h. The samples were centrifuged at 1500 rpm for 10 min at 4 °C, and 100 μL of supernatant from each sample was transferred into a 96-well plate. The release of hemoglobin was determined by the absorbance at 540 nm using a microplate reader. RBCs treated with Triton X-100 (2%) and DPBS were considered as the positive and negative controls, respectively. Hemoglobin release was calculated as $(OD_{sample} - OD_{negative\ control})/(OD_{positive\ control} - OD_{negative\ control}) \times 100\%$.

In Vitro Cell Cytotoxicity. DU145 (2000 cells/well), PC-3 (5000 cells/well), MDA-MB-231 (2000 cells/well), or 4T1 (1000 cells/well) were seeded in 96-well plates followed by 24 h of incubation in DMEM with 10% FBS and 1% streptomycin–penicillin. Then, various concentrations of PTX (dissolved in DMSO or formulated in $PEG_{3.5K}$-EB_2 micelles) were added in quadruplicate and cells were incubated for 72 h. 20 μL of 3-(4, 5-dimethylthiazol-2-yl)-2,5-diphenyltetrazolium-bromide (MTT) in PBS (5 mg/mL) was added and cells were further incubated for 4 h. The medium in the plates was removed and MTT formazan was solubilized by DMSO. The absorbance was measured by microplate reader with wavelength at 550 nm and reference wavelength at 630 nm. Untreated groups were used as controls. Cell viability was calculated as $[(OD_{treat} - OD_{blank})/(OD_{control} - OD_{blank}) \times 100\%]$.

RESULTS

Synthesis of $PEG_{3.5K}$-EB_2 Conjugates. We have developed a strategy to synthesize $PEG_{3.5K}$-EB_2 conjugate in which two molecules of embelin were coupled to one molecule of PEG via a linker of aspartic acid. This is modified from the scheme reported by Wang's group[27] for the total synthesis of embelin. This involves the synthesis of benzoquinone followed by coupling to carboxyl groups of aspartic acid. Undecyl side chains were then installed onto each of the two benzoquinone rings. Finally, PEG was coupled to aspartic acid-EB_2 through the deprotected amino group. HPLC shows that the purity of the final product ($PEG_{3.5K}$-EB_2) is 94% (Figure S1). ^{1}H NMR spectrum of $PEG_{3.5K}$-EB_2 shows signals at 3.63 ppm attributable to the methylene protons of PEG, the embelin proton signals at 8.14 and 6.72 ppm, and the carbon chain singles at 1.05–1.25 ppm. The aspartate signals were identified at 5.57, 4.98, and 2.60 ppm (Figure S2). The molecular weight of the $PEG_{3.5K}$-EB_2 conjugate from MALDI-TOF MS (4197) is very similar to the theoretical value (4203) (Figure S3). These results suggest successful synthesis of $PEG_{3.5K}$-EB_2 conjugate.

Biophysical Characterization of Micelles. Micelles were readily prepared from $PEG_{3.5K}$-EB_2 conjugate via solvent evaporation method. $PEG_{3.5K}$-EB_2 conjugate can be dissolved in water at concentration up to 750 mg/mL (data not shown). Dynamic light scattering (DLS) measurements showed that these micelles had hydrodynamic sizes around 22 nm at the

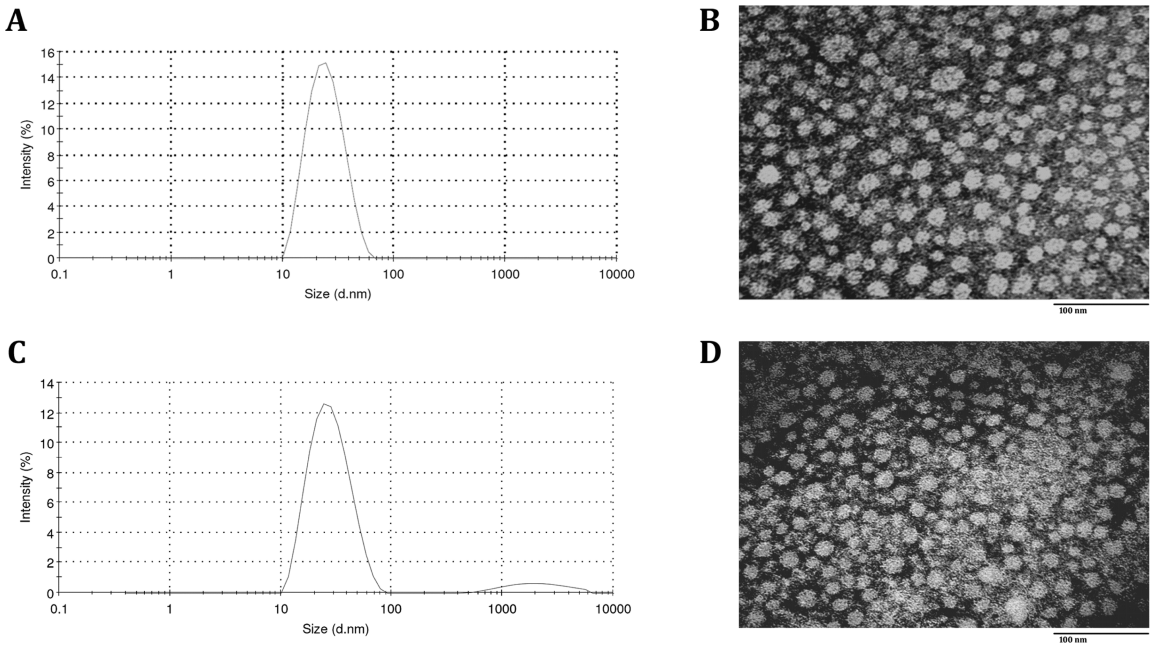

Figure 1. Particle size distribution of $PEG_{3.5K}$-EB_2 (A) and PTX-loaded $PEG_{3.5K}$-EB_2 (C). TEM images of self-assembled micelles of $PEG_{3.5K}$-EB_2 (B) and PTX-loaded $PEG_{3.5K}$-EB_2 (D). The spherical micelles with the diameter of around 20 nm were observed. The drug loading level was 1 mg/mL (PTX) in $PEG_{3.5K}$-EB_2.

concentration of 20 mg/mL (Figure 1A), which shall ensure efficient passive targeting to the solid tumors.

PTX, a potent hydrophobic anticancer agent, was readily loaded into $PEG_{3.5K}$-EB_2 micelles. Figure 1C shows the DLS size measurement of PTX-loaded $PEG_{3.5K}$-EB_2 micelles at a drug concentration of 1 mg/mL. There were minor changes in sizes when PTX was loaded into micelles at a carrier/drug ratio of 7.5/1 (m/m).

Figure 1B,D shows the TEM images of drug-free and PTX-loaded micelles after staining with 1% uranyl acetate. Spherical particles of uniform size were observed for both drug-free and PTX-loaded micelles. The sizes of the micelles observed under TEM are consistent with those measured by DLS.

Table 1 shows the sizes of PTX-loaded micelles at different carrier/drug molar ratios. PTX-loaded $PEG_{3.5K}$-EB_2 micelles had relatively large size (~143 nm) at a carrier/drug ratio of 2.5: 1 (m/m) and the particles were stable for less than 1 day. Increasing the input molar ratio of $PEG_{3.5K}$-EB_2/PTX led to gradual decrease in the size of PTX-loaded micelles. At the molar ratio of 7.5/1, the size of the PTX-loaded micelles was similar to that of drug-free micelles.

Table 1. DLS Analysis of the Sizes of Free and Drug-Loaded $PEG_{3.5K}$-EB_2 Micelles[a]

micelles	molar ratio	size[b] (nm)	PDI[c]
$PEG_{3.5K}$-EB_2	—	22.8 ± 0.3	0.09
$PEG_{3.5K}$-EB_2:PTX[d]	2.5:1	143 ± 17	0.23
$PEG_{3.5K}$-EB_2:PTX	5:1	58.7 ± 0.5	0.32
$PEG_{3.5K}$-EB_2:PTX	7.5:1	27.5 ± 0.2	0.23

[a]PTX concentration in micelle was kept at 1 mg/mL. Blank micelle concentration was 20 mg/mL. Values repotted are the mean ± SD for triplicate samples. [b]Measured by dynamic light scattering particle sizer (Zetasizer). [c]PDI = polydispersity index. [d]PTX = paclitaxel.

Drug Loading Efficiency (DLE). DLE of PTX-loaded micelles were determined by HPLC and the results are shown in Table 2. DLE was as high as 79.89% when PTX was formulated in $PEG_{3.5K}$-EB_2 micelles at a carrier/PTX input ratio of 2.5/1 (m/m) and PTX concentration of 1.07 mg/mL. Increasing the carrier/PTX input ratios led to further increase in DLE. $PEG_{3.5K}$-EB_2/PTX formed the most stable particles at a carrier/drug ratio of 7.5/1. At this ratio, PTX was quantitatively formulated in the $PEG_{3.5K}$-EB_2 micelles when the PTX concentration was less than 2.14 mg/mL. Increasing the PTX concentration to 3.21 mg/mL led to a slight decrease in DLE (81.3%). The surface charges of PTX-loaded $PEG_{3.5K}$-EB_2 micelles were close to neutral (+1.89 to −2.64) for all particles examined.

Table 2. Physicochemical Characterization of PTX-Loaded PPEG$_{3.5K}$-EB_2 Micelles[a]

$PEG_{3.5K}$-EB_2:PTX (m/m)	concentration of PTX in micelles (mg/mL)	DLC[b] (%)	DLE[c] (%)	zeta[d] (mV)
2.5:1	1.07	7.51	79.9	1.58 ± 0.37
5:1	1.07	3.90	96.7	1.89 ± 0.08
7.5:1	1.07	2.63	98.6	−1.52 ± 0.20
	2.14	2.63	97.5	−1.29 ± 0.19
	3.21	2.63	81.3	−2.64 ± 0.43

[a]Values reported are the means ± SD for triplicate samples. [b]DLC = drug loading capacity. [c]DLE = drug loading efficiency. [d]Measured by dynamic light scattering particle sizer (Zetasizer).

CMC Measurements. Figure 2 shows the results of CMC measurements using pyrene as a fluorescence probe. Upon incorporation into the micelles, the fluorescence intensity of pyrene increases substantially at the concentration of micelles above the CMC.[28] On the basis of the partition of the pyrene, the CMC of $PEG_{3.5K}$-EB_2 could be obtained by plotting the fluorescence intensity versus logarithm concentration of the polymer. The CMC of $PEG_{3.5K}$-EB_2 was determined from the crossover point at the low concentration range. The CMC of

dx.doi.org/10.1021/bc3000468 | Bioconjugate Chem. 2012, 23, 1443−1451

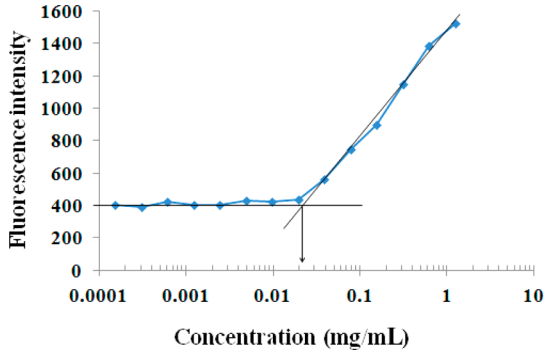

Figure 2. CMC measurement of the $PEG_{3.5K}$-EB_2 micelles using pyrene as a hydrophobic fluorescence probe. The fluorescence intensity of pyrene was collected at the excitation wavelength of 334 nm and the emission wavelength of 390 nm. The fluorescence intensity was plotted as a function of logarithmic concentration of $PEG_{3.5K}$-EB_2 micelles, [pyrene] = 6×10^{-7} mol/L. Values reported are the means ± SD for triplicate samples.

the $PEG_{3.5K}$-EB_2 conjugate is 4.9 μM, which is similar to most reported micellar delivery systems.

Hemolysis Study. One of the safety concerns for polymeric micelle systems is the hemolytic activity. To address this issue, the hemolytic activity of drug-free $PEG_{3.5K}$-EB_2 micelles was examined and compared to a strong detergent Triton X-100 and polyethylenimine (PEI), a cationic polymer known to have significant hemolytic effect.[29] As shown in Figure 3, PEI

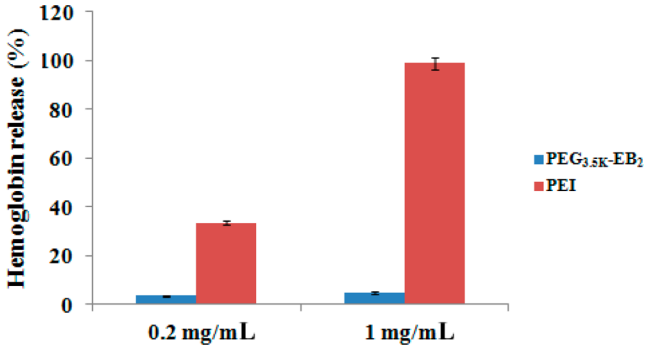

Figure 3. In vitro hemolysis assay of $PEG_{3.5K}$-EB_2 compared with PEI. Both $PEG_{3.5K}$-EB_2 and PEI with two different concentrations [0.2, 1 mg/mL) were incubated with rat red blood cells (RBCs) for 4 h at 37 °C in an incubator shaker. The degree of RBCs lysis was measured spectrophotometrically (λ = 540 nm) according to the release of hemoglobin in process (2% Triton X-100 and DPBS were used as a positive and negative control, respectively). Values reported are the means ± SD for triplicate samples.

induced hemolysis in a dose-dependent manner. In contrast, no observable hemolytic activities (<5%) were found for $PEG_{3.5K}$-EB_2 micelles, suggesting the excellent safety of our new delivery system.

In Vitro Cytotoxicity. Figure 4 shows the cytotoxicity of $PEG_{3.5K}$-EB_2 in comparison with free embelin (dissolved in DMSO) in 3 cancer cell lines tested including murine breast cancer cells 4T1, and two human prostate cancer cell lines PC3 and DU145. $PEG_{3.5K}$-EB_2 was comparable to free embelin in antitumor activity in all 3 cancer cell lines with IC_{50} in the low micromolar range.

Figure 5A compares the cytotoxicity of free PTX (in DMSO) to that of $PEG_{3.5K}$-EB_2-formulated PTX (5/1, m/m) in MDA-MB-231 cells. Drug-free $PEG_{3.5K}$-EB_2 did not cause any cytotoxicity to MDA-MB-231 cells due to its relatively low concentrations used in this study. Free PTX exhibited cytotoxicity on MDA-MB-231 cells in a dose-dependent manner. However, formulation of PTX in $PEG_{3.5K}$-EB_2 micelles resulted in a significant increase in the cytotoxicity. Similar results were found with three other cancer cell lines (Figure 5B–D). Table 3 summarizes the IC_{50} of free PTX and $PEG_{3.5K}$-EB_2-formulated PTX in the four different cancer cell lines. Depending on the cell lines, the IC_{50} was decreased by 1.5- to 8.7-fold when PTX was formulated in $PEG_{3.5K}$-EB_2 micelles.

DISCUSSION

We have developed a new delivery system that consists of an embelin-based hydrophobic domain and a PEG hydrophilic segment. The $PEG_{3.5K}$-EB_2 conjugate readily forms micelles in aqueous solutions. More importantly, hydrophobic drugs such as PTX can be loaded into $PEG_{3.5K}$-EB_2 micelles.

Various polymeric micelle systems have been reported. Most micellar systems consist of a hydrophobic core that does not have any potential therapeutic effect.[30] In addition, the metabolites of the hydrophobic segments might contribute to some undesired effects, such as inflammation and systemic toxicity.[30,31] The $PEG_{3.5K}$-EB_2 conjugate developed in this study represents a dual-functional delivery system that may overcome these limitations. Embelin is a natural product that demonstrates various biological effects including antitumor activity.[15] Embelin also shows excellent safety profiles in animals.[32] Thus, PEG-derivatized embelin may be an attractive delivery system to achieve synergistic activity with anticancer agents while minimizing the carrier-associated toxicity. PEG–embelin conjugates can be synthesized via direct coupling of embelin to PEG via an ester linkage. However, such synthesis is likely to yield a mixture of products with PEG randomly linked to the different hydroxyl groups in the benzene ring. We have developed a strategy to generate $PEG_{3.5K}$-EB_2 conjugate via total synthesis (Scheme 1). This method was modified from a scheme reported by Wang's group for total synthesis of embelin.[27] Our synthesis ensures generation of a structurally well-defined conjugate in which PEG is attached to 1-OH group in the quinone ring. Most of the steps give good yields, and the synthesis of PEG–embelin conjugate involves a similar number of steps and cost as that of embelin alone.[27]

$PEG_{3.5K}$-EB_2 conjugate forms small-sized micelles (20–30 nm), and loading of PTX did not significantly affect the size of the micelles. It was generally believed that particles in the size range 100–200 nm can effectively penetrate solid tumors via an EPR effect.[6] A recent study from Lam's group compared the passive targeting of nanoparticles of different sizes in a subcutaneous model of human ovarian cancer xenograft. It was shown that particles with a size of 154 nm were significantly taken up by liver and lungs with limited accumulation at tumor sites. In contrast, particles with respective size of 17 and 64 nm were much more effective in passive targeting to the solid tumor.[33] Cabral and colleagues compared the targeting efficiency of polymeric micelles of different sizes (30, 50, 70, and 100 nm) in both highly and poorly permeable tumors. While all of the tested polymer micelles penetrated highly permeable tumors in mice, only the 30 nm micelles could penetrate poorly permeable pancreatic tumors to achieve an antitumor effect.[34] The small size of our new micelle system suggests its potential for effective tumor

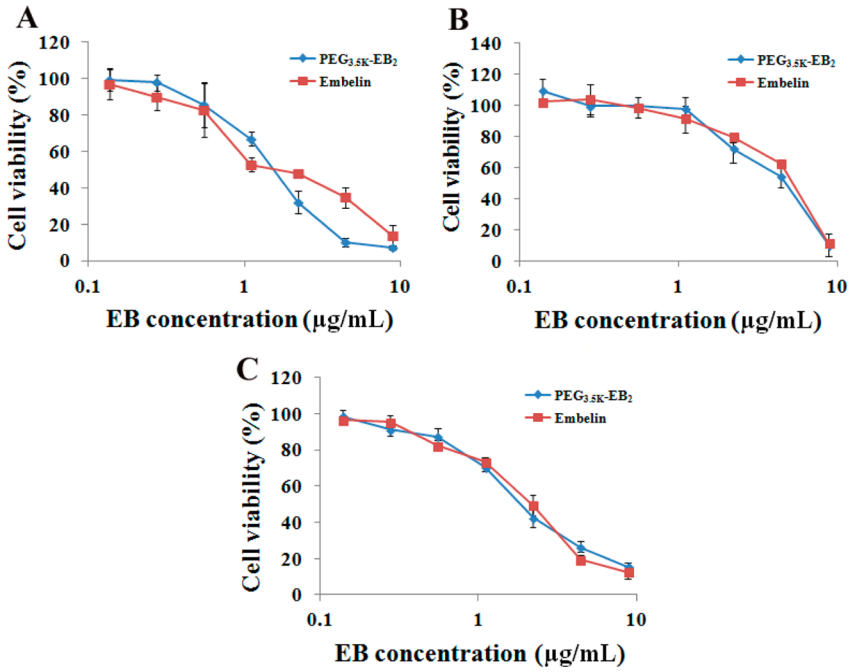

Figure 4. Cytotoxicity of free EB and $PEG_{3.5K}$-EB_2 against the 4T1 mouse breast cancer cell line (A) and two androgen-independent human prostate cancer cell lines PC-3 (B) and DU145 (C). Cells were treated by free EB or $PEG_{3.5K}$-EB_2 for 72 h under the equivalent concentrations of EB. Cytotoxicity was determined by MTT assay.

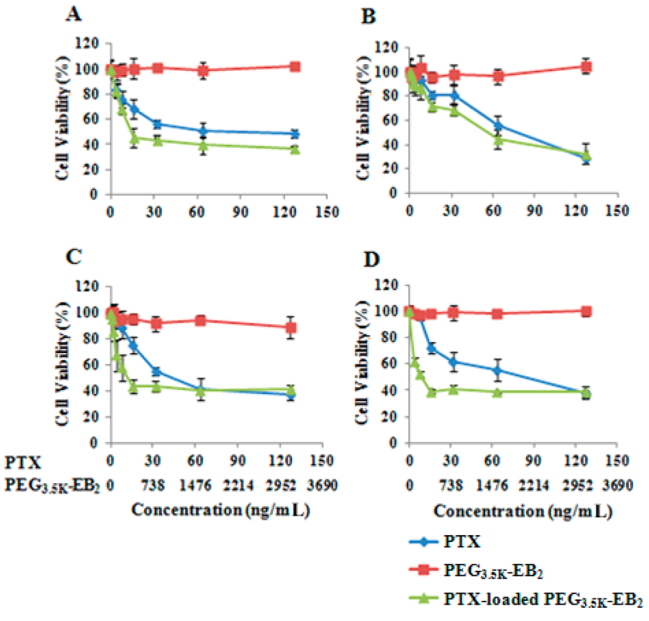

Figure 5. Cytotoxicity of free PTX, free $PEG_{3.5K}$-EB_2, and PTX-loaded $PEG_{3.5K}$-EB_2 (1/5, m/m) nanoparticles against the MDA-MB-231 human breast cancer cell line (A), the 4T1 mouse breast cancer cell line (B), and two androgen-independent human prostate cancer cell lines PC-3 (C) and DU145 (D). Cells were treated with free or formulated PTX for 72 h and cytotoxicity was determined by MTT assay.

targeting in vivo, which is currently being evaluated in our laboratory.

In vitro cytotoxicity with several cancer cell lines showed that $PEG_{3.5K}$-EB_2 is comparable to free embelin in antitumor activity with IC_{50} in the low micromolar range. More importantly, $PEG_{3.5K}$-EB_2 synergizes with PTX in antitumor activity at much lower concentrations (~nM) in all 4 cancer cell lines tested.

Table 3. IC_{50} of PTX and PTX-Loaded $PEG_{3.5K}$-EB_2 (1/5, m/m) after 72 h Incubation with Different Cancer Cell Lines

	IC_{50}[a] (ng/mL)			
	MDA-MB-231	4T1	PC-3	DU145
PTX-loaded $PEG_{3.5K}$-EB_2	13.5	51	12.7	8.9
PTX	65	73	42.3	78

[a]The concentration of a drug that is required for 50% inhibition in vitro.

The $PEG_{3.5K}$-EB_2-mediated cytotoxicity is unlikely attributed to its surface activity, as $PEG_{3.5K}$-EB_2 showed minimal hemolytic activity even at mM concentrations (Figure 3). Embelin is coupled to PEG via a cleavable ester linkage. It is likely that embelin is released from the conjugate following intracellular delivery and executes the antitumor effect by itself or synergizes with PTX in antitumor activity. These data are consistent with the observation that free embelin synergizes with PTX at subeffective doses (Figure S4). More studies are needed to better understand the mechanism by which the $PEG_{3.5K}$-EB_2-based delivery system synergizes with PTX in vitro.

It should be noted that $PEG_{3.5K}$-EB_2 conjugate only represents a model micelle to demonstrate the utility of PEG-derivatized embelin as a dual functional delivery system for hydrophobic anticancer drugs. Considering the flexibility of our synthesis scheme, more studies on structure–activity relationship (SAR) can be designed to further improve this new delivery system. These include optimization of the molar ratio of PEG/embelin in the conjugates, the length and structure of the acyl chain in the embelin, and the molecular weight of PEG. Recently, embelin derivatives with improved affinity toward XIAP have been developed.[27] The utility of these new derivatives as drug carriers can also be examined and compared to native embelin. Finally, promising candidates identified from these studies need to be further evaluated in vivo. These studies are currently ongoing in our laboratory.

dx.doi.org/10.1021/bc3000468 | Bioconjugate Chem. 2012, 23, 1443–1451

■ ASSOCIATED CONTENT

Supporting Information

HPLC trace, ^{1}H NMR spectra, and MALDI-TOF of $PEG_{3.5K}$-EB_2, and the cytotoxicity of embelin, PTX, and the combination of embelin and PTX against human prostate cancer cells DU145. This material is available free of charge via the Internet at http://pubs.acs.org.

■ AUTHOR INFORMATION

Corresponding Author

*Tel: 412-383-7976. Fax: 412-648-1664. E-mail: sol4@pitt.edu.

Author Contributions

#Authors contributed equally to this work.

Notes

The authors declare no competing financial interest.

■ ACKNOWLEDGMENTS

This work was supported in part by NIH grants R21CA128415 and R21CA155983, and a DOD grant BC09603. We would like to thank Dr. Gong Chen at Penn State University for critical reading of this manuscript.

■ REFERENCES

(1) Paál, K., Müller, J., and Hegedûs, L. (2001) High affinity binding of paclitaxel to human serum albumin. *Eur. J. Biochem. 268*, 2187−2191.

(2) Xie, Z., Guan, H., Chen, X., Lu, C., Chen, L., Hu, X., Shi, Q., and Jing, X. (2007) A novel polymer-paclitaxel conjugate based on amphiphilic triblock copolymer. *J. Controlled Release 117*, 210−216.

(3) Torchilin, V. P. (2007) Micellar nanocarriers: pharmaceutical perspectives. *Pharm. Res. 24*, 1−16.

(4) Sutton, D., Nasongkla, N., Blanco, E., and Gao, J. (2007) Functionalized micellar systems for cancer targeted drug delivery. *Pharm. Res. 24*, 1029−1046.

(5) Mi, Y., Liu, Y., and Feng, S. S. (2011) Formulation of docetaxel by folic acid-conjugated D-a-tocopheryl polyethylene glycol succinate 2000 (Vitamin E $TPGS_{2k}$) micelles for targeted and synergistic chemotherapy. *Biomaterials 32*, 4058−4066.

(6) Matsumura, Y., and Maeda, H. (1986) A new concept for macromolecular therapeutics in cancer chemotherapy: mechanism of tumouritropic accumulation of proteins and the antitumour agent smancs. *Cancer Res. 46*, 6387−6392.

(7) Gao, Z., Lukyanov, A. N., Singhal, A., and Torchilin, V. P. (2002) Diacyllipid-polymer micelles as nanocarriers for poorly soluble anticancer drugs. *Nano Lett. 2*, 979−982.

(8) Croy, S. R., and Kwon, G. S. (2006) Polymeric micelles for drug delivery. *Curr. Pharm. Des. 12*, 4669−4684.

(9) Dong, Y., and Feng, S. S. (2005) Poly(d,l-lactide-co-glycolide)/montmorillonite nanoparticles for oral delivery of anticancer drugs. *Biomaterials 30*, 6068−6076.

(10) Zhang, Z., and Feng, S. S. (2006) Nanoparticles of poly(lactide)/vitamin E TPGS copolymer for cancer chemotherapy: synthesis, formulation, characterization and in vitro drug release. *Biomaterials 27*, 262−270.

(11) Zhang, Z., Lee, S. H., Gan, C. W., and Feng, S. S. (2008) In vitro and in vivo investigation on PLA-TPGS nanoparticles for controlled and sustained small molecule chemotherapy. *Pharm. Res. 8*, 1925−1935.

(12) Prashant, C., Dipak, M, Yang, C. T., Chuang, K. H., Jun, D., and Feng, S. S. (2010) Superparamagnetic iron oxide--loaded poly(lactic acid)-D-alpha-tocopherol polyethylene glycol 1000 succinate copolymer nanoparticles as MRI contrast agent. *Biomaterials 31*, 5588−5597.

(13) Ji, X., Wang, Z., Geamanu, A., Sarkar, F. H., and Gupta, S. V. (2011) Inhibition of cell growth and induction of apoptosis in non-small cell lung cancer cells by delta-tocotrienol is associated with notch-1 down-regulation. *J. Cell. Biochem. 112*, 2773−2783.

(14) Husain, K., Francois, R. A., Yamauchi, T., Perez, M., Sebti, S. M., and Malafa, M. P. (2011) Vitamin E δ-Tocotrienol augments the antitumor activity of gemcitabine and suppresses constitutive NF-κB activation in pancreatic cancer. *Mol. Cancer Ther. 10*, 2363−2372.

(15) Chitra, M., Sukumar, E., Suja, V., and Devi, C. S. (1994) Antitumor, anti-inflammatory and analgesic property of embelin, a plant product. *Chemotherapy 40*, 109−113.

(16) Bhandari, U., Jain, N., and Pillai, K. K. (2007) Further studies on antioxidant potential and protection of pancreatic beta-cells by Embelia ribes in experimental diabetes. *Exp. Diabetes Res. 2007*, 15803−15808.

(17) Singh, D., Singh, R., Singh, P., and Gupta, R. S. (2009) Effect of embelin on lipid peroxidation and free radical scavenging activity against liver damage in rats. *Basic Clin. Pharmacol. Toxicol. 105*, 243−248.

(18) Danquah, M., Li, F., Duke, C. B., Miller, D. D., and Mahato, R. I. (2009) Micellar delivery of bicalutamide and embelin for treating prostate cancer. *Pharm. Res. 26*, 2081−2092.

(19) Sreepriya, M., and Bali, G. (2005) Chemopreventive effects of embelin and curcumin against N-nitrosodiethylamine/phenobarbital-induced hepatocarcinogenesis in Wistar rats. *Fitoterapia 76*, 549−555.

(20) Dai, Y., Qiao, L., Chan, K. W., Yang, M., Ye, J., Ma, J., Zou, B., Gu, Q., Wang, J., Pang, R., Lan, H. Y., and Wong, B. C. (2009) Peroxisome proliferator-activated receptor-gamma contributes to the inhibitory effects of Embelin on colon carcinogenesis. *Cancer Res. 69*, 4776−4783.

(21) Heo, J. Y., Kim, H. J., Kim, S. M., Park, K. R., Park, S. Y., Kim, S. W., Nam, D., Jang, H. J., Lee, S. G., Ahn, K. S., Kim, S. H., Shim, B. S., Choi, S. H., and Ahn, K. S. (2011) Embelin suppresses STAT3 signaling, proliferation, and survival of multiple myeloma via the protein tyrosine phosphatase PTEN. *Cancer Lett. 308*, 71−80.

(22) Nikolovska-Coleska, Z., Xu, L., Hu, Z., Tomita, Y., Li, P., Roller, P. P., Wang, R., Fang, X., Guo, R., Zhang, M., Lippman, M. E., Yang, D., and Wang, S. (2004) Discovery of embelin as a cell-permeable, small-molecular weight inhibitor of XIAP through structure-based computational screening of a traditional herbal medicine three-dimensional structure database. *J. Med. Chem. 47*, 2430−2440.

(23) Tamm, I., Kornblau, S. M., Segall, H., Krajewski, S., Welsh, K., Kitada, S., Scudiero, D. A., Tudor, G., Qui, Y. H., Monks, A., Andreeff, M., and Reed, J. C. (2000) Expression and prognostic significance of IAP-family genes in human cancers and myeloid leukemias. *Clin. Cancer Res. 6*, 1796−1803.

(24) Holcik, M., Gibson, H., and Korneluk, R. G. (2001) XIAP: apoptotic brake and promising therapeutic target. *Apoptosis 6*, 253−261.

(25) Ahn, K. S., Sethi, G., and Aggarwal, B. B. (2007) Embelin, an inhibitor of X chromosome-linked inhibitor-of-apoptosis protein, blocks nuclear factor-kappaB (NF-kappaB) signaling pathway leading to suppression of NF-kappaB-regulated antiapoptotic and metastatic gene products. *Mol. Pharmacol. 71*, 209−219.

(26) La, S. B., Okano, T., and Kataoka, K. (1996) Preparation and characterization of the micelle-forming polymeric drug indomethacin-incorporated poly(ethylene oxide)-poly(beta-benzyl L-aspartate) block copolymer micelles. *J. Pharm. Sci. 85*, 85−90.

(27) Chen, J., Nikolovska-Coleska, Z., Wang, G., Qiu, S., and Wang, S. (2006) Design, synthesis, and characterization of new embelin derivatives as potent inhibitors of X-linked inhibitor of apoptosis protein. *Bioorg. Med. Chem. Lett. 16*, 5805−5808.

(28) Kabanov, A. V., Nazarova, I. R., Astafieva, I. V., Batrakova, E. V., Alakhov, V. Y., Yaroslavov, A. A., and Kabanov, V. A. (1995) Micelle formation and solubilization of fluorescent probes in poly-(oxyethylene-b-oxypropylene-b-oxyethylene) solutions. *Macromolecules 28*, 2303−2314.

(29) Reul, R., Nguyen, J., and Kissel, T. (2009) Amine-modified hyperbranched polyesters as non-toxic, biodegradable gene delivery systems. *Biomaterials 30*, 5815−5824.

(30) Li, G., Liu, J., Pang, Y., Wang, R., Mao, L., Yan, D., Zhu, X., and Sun, J. (2011) Polymeric micelles with water-insoluble drug as

hydrophobic moiety for drug delivery. *Biomacromolecules 12*, 2016−2026.
(31) Tang, N., Du, G., Wang, N., Liu, C., Hang, H., and Liang, W. (2007) Improving penetration in tumors with nanoassemblies of phospholipids and doxorubicin. *J. Natl. Cancer Inst. 99*, 1004−1015.
(32) Kumar, G, K., Dhamotharan, R., Kulkarni, N. M., Honnegowda, S., and Murugesan, S. (2011) Embelin ameliorates dextran sodium sulfate-induced colitis in mice. *Int. Immunopharmacol. 11*, 724−731.
(33) Luo, J., Xiao, K., Li, Y., Lee, J. S., Shi, L., Tan, Y. H., Xing, L., Cheng, R. H., Liu, G. Y., and Lam, K. S. (2010) Well-defined, size-tunable, multifunctional micelles for efficient paclitaxel delivery for cancer treatment. *Bioconjugate Chem. 21*, 1216−1224.
(34) Cabral, H., Matsumoto, Y., Mizuno, K., Chen, Q., Murakami, M., Kimura, M., Terada, Y., Kano, M. R., Miyazono, K., Uesaka, M., Nishiyama, N., and Kataoka, K. (2011) Accumulation of sub-100 nm polymeric micelles in poorly permeable tumours depends on size. *Nat. Nanotechnol. 6*, 815−823.